Pediatr Radiol (2012) 42:1235–1249
DOI 10.1007/s00247-012-2439-6

PICTORIAL ESSAY

Imaging features of pediatric musculoskeletal tuberculosis

Akhila Prasad · Smita Manchanda · Namrita Sachdev · Barindra Prasad Baruah · Vivek Manchanda

Received: 9 October 2011 / Revised: 29 April 2012 / Accepted: 4 May 2012 / Published online: 27 June 2012

Abstract Tuberculosis (TB) is widely prevalent in developing nations and has recently made a comeback in industrialized countries, with the rise in immunocompromized patients. Musculoskeletal TB in children presents a diagnostic challenge because it is difficult to recognize in the early stages of the disease, and imaging features mimic other entities. The clinical onset is insidious, with an indolent course and a resultant late presentation. It leads to significant morbidity; a delay in diagnosis can cause potentially serious neurological complications and bone and joint destruction. Conventional radiographs are the initial imaging modality and US, CT and MRI are used in conjunction to better delineate the disease extent and morphology. Radiologists should be familiar with the spectrum of imaging features of TB, including plain radiographs and MRI, and aid the clinician in making an early diagnosis. Aspiration or biopsy with examination for acid-fast bacillus and histological evaluation is required to confirm the diagnosis.

Keywords Tuberculosis · Spondylitis · Arthritis · Osteomyelitis · Children

A. Prasad (✉) · S. Manchanda · N. Sachdev · B. P. Baruah
Department of Radiodiagnosis, PGIMER and Dr RML Hospital,
C-6/43/2, Safdarjung Development Area,
New Delhi, India 110016
e-mail: akhil43@yahoo.com

V. Manchanda
Department of Pediatric Surgery, Chacha Nehru Bal Chikitsalaya,
New Delhi, India

Introduction

Tuberculosis (TB) is a common disease entity, especially in developing countries. There has been a resurgence in the incidence of TB in developed nations, with a growing number of immigrant populations, increased numbers of immunocompromized patients, changing elderly population demographics, multidrug-resistant TB and various socioeconomic factors (e.g., poverty, alcohol and drug abuse) [1–3]. According to an estimate by the World Health Organization (WHO), 3 million people a year worldwide die due to TB. India is estimated to have one-fifth of the world's TB patients with an estimated 6 million radiologically proven cases [4].

Extrapulmonary manifestations are seen in approximately 20% of patients with TB [5]. Musculoskeletal TB accounts for 1–3% of tuberculous infections, with coexistent active pulmonary TB in less than half of these patients [6, 7]. The demographic profile varies, with skeletal TB being more common in children in Asia and Africa and in adults in North America [8]. The diagnosis of TB in children is a challenge because early manifestations are subtle and advanced disease can be confused with other pathologies such as tumors or trauma [2, 9]. A high degree of clinical suspicion is required for an early diagnosis, though elevated erythrocyte sedimentation rate (ESR) and positive tuberculin skin test may be contributory. Identifying the common and uncommon radiologic findings can help in accurate diagnosis and early treatment to prevent complications [10]. MRI of the musculoskeletal system is now performed routinely and it is important to be able to recognize the MR imaging features suggestive of TB. Image-guided sampling can also be used to obtain histopathological confirmation [11].

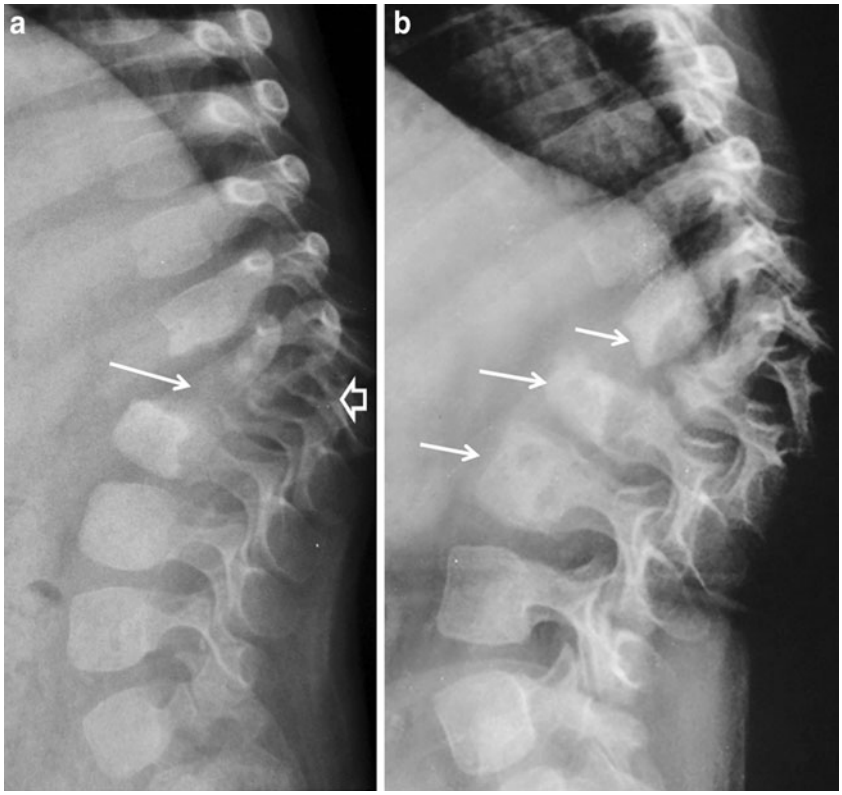

Fig. 1 Tuberculosis of the thoracolumbar spine in a 4-year-old girl. **a** Initial radiograph shows partial collapse of T12, L1 and L2 vertebral bodies (*arrow*) with kyphotic deformity. The posterior elements are intact (*open arrow*). **b** Radiograph obtained 6 months later shows progression of the disease with new lytic lesions (*arrows*) in the T11, L3 and L4 vertebral bodies. There was noncompliance with treatment

The most common form of musculoskeletal TB in adults and children is tuberculous spondylitis, which accounts for more than 50% of the cases [12]. The other 50% of cases are extraspinal manifestations, of which peripheral arthritis accounts for 60%, osteomyelitis 38% and tenosynovitis and bursitis 2% [13–15].

In this article, we illustrate the common radiologic manifestations of musculoskeletal tuberculosis in children.

Tuberculous spondylitis

Also known as Pott disease, tuberculous spondylitis was first described by Sir Percival Pott in 1779 [2]. The usual clinical manifestations include persistent spinal pain, tenderness, limitation of mobility and constitutional symptoms [16].

Spread of infection is usually hematogenous by perivertebral arterial plexus or venous plexus of Batson, or rarely by contiguous spread from a paraspinal infection [2].

The infection begins at the superior or inferior anterior vertebral body corner in the paradiscal location. Further spread can occur via subligamentous route or through the subchondral plate. Disc involvement is seen late with narrowing secondary to herniation of the disc into the collapsed vertebral body. Collapse of multiple vertebrae with anterior wedging leads to the gibbus deformity. In children, the "tall vertebrae" may be seen because the disease occurs during the growth period (before the disappearance of the growth zone) [4].

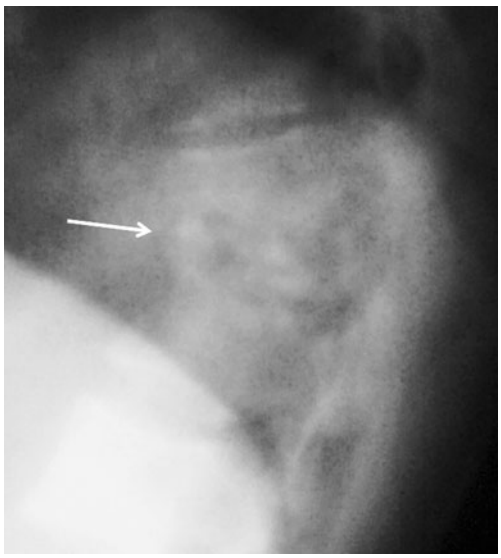

Fig. 2 TB of the spine in a 17-year-old boy. Lateral radiograph of the thoracic spine reveals irregular lytic destruction of T9 and T10 vertebra and loss of intervening disc space (*arrow*)

Exudates in the soft tissues track as abscesses in the pre- and paravertebral space, epidural space and along the fascial planes [17]. A psoas abscess may extend into the groin and thigh and calcification may be seen in a healed psoas abscess [18].

Tuberculous spondylitis in adults most frequently affects the thoracolumbar junction, but pediatric case series have reported the thoracic spine to be most commonly involved [18–20]. In children, vertebral body involvement is more often central with collapse commencing anteriorly. Subsequent spread through the vertebra may lead to collapse. When there is complete destruction of the vertebral body, diagnosis can be made by noting the lack of vertebral body against the visualized posterior elements. This helps to determine the site of involvement and the number of vertebral bodies destroyed [20]. Multiple contiguous vertebral bodies are usually involved; however, skip lesions have also been described. Pediatric cases usually have two or more vertebrae involved—likely due to late presentation or severe manifestation with more rapid penetration of the relative barrier that the discs provide.

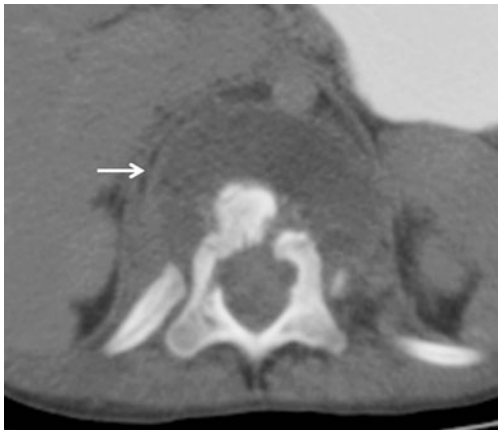

Fig. 4 Postcontrast axial CT scan of a 5-year-old boy shows fragmentary destruction of the vertebral body with associated pre- and paravertebral abscess (*arrow*)

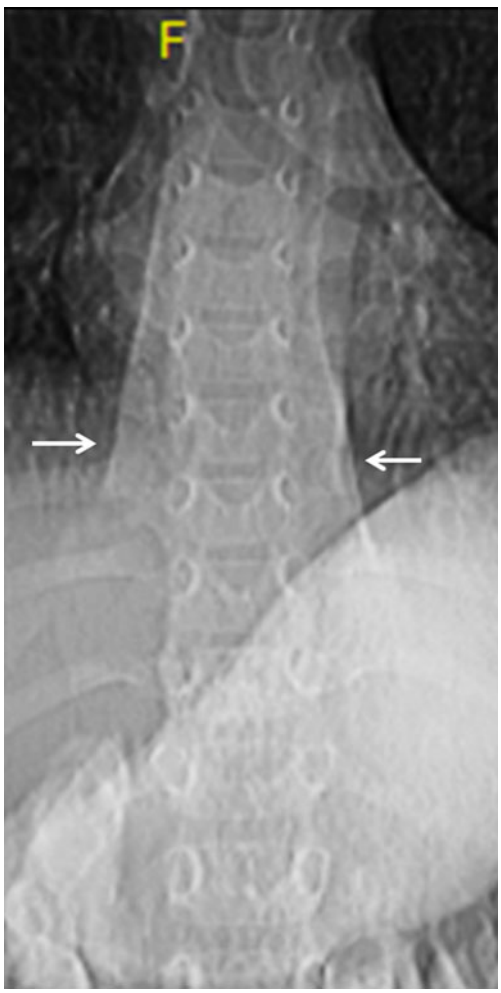

Fig. 3 CT scanogram of thoracic spine shows a characteristic petering abscess (between *arrows*) with indistinct inferior margins in a 5-year-old boy with thoracic spine TB

The following types of tuberculous involvement of the spine have been described: paradiscal, anterior subperiosteal, central and appendiceal [19]. Paradiscal or the marginal type is the most common type. Infection starts at the end plates with subsequent involvement of the vertebral body. In the central type, there is a lytic area in the center of the vertebral body. Initial expansion is followed by a concentric collapse resembling vertebra plana. In the anterior subperiosteal type, infection starts beneath the periosteum at the anterior vertebral margin and spreads underneath the anterior longitudinal ligament. Isolated involvement of the

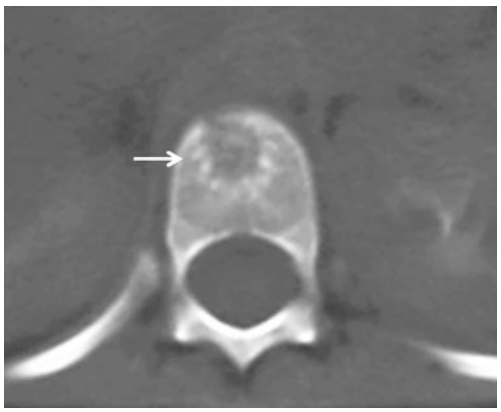

Fig. 5 Axial CT scan of a 7-year-old girl with TB of the thoracic spine shows an osteolytic lesion in the anterior vertebral body (*arrow*)

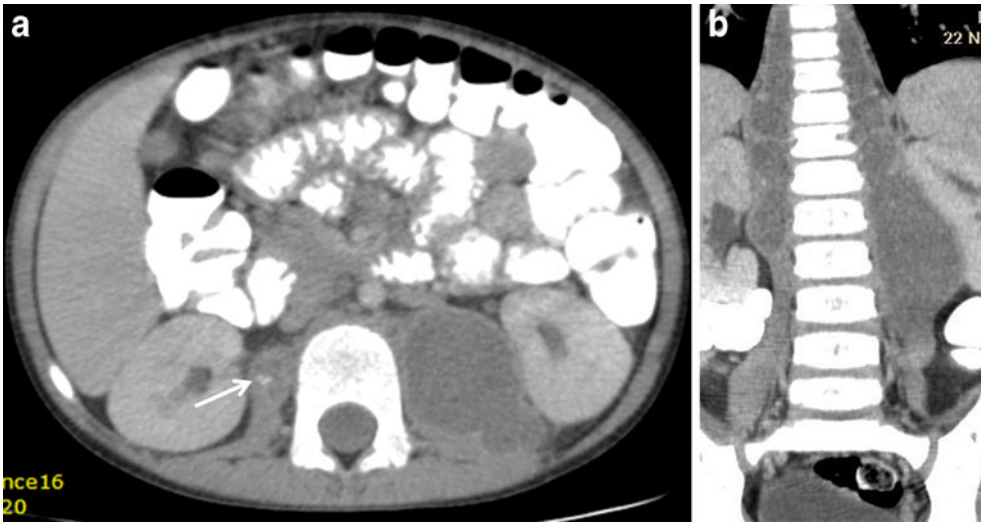

Fig. 6 Axial (**a**) and coronal (**b**) reformatted contrast-enhanced CT images of the same patient as in Fig. 3 show bilateral paravertebral and psoas abscesses. A small speck of calcification is seen in the right psoas abscess (*arrow* in **a**)

posterior elements resulting in appendiceal or neural arch tuberculosis (NAT) is rare, with less than 2% of all cases of spinal TB in nonendemic areas and 5% to 10% in endemic areas in adults [21]. In children, posterior element involvement is commonly an extension of the vertebral body disease with isolated neural arch tuberculosis rarely reported.

Plain radiography is believed to be the mainstay of diagnosis as it provides most of the information necessary for diagnosis and treatment of spinal TB in children [20]. Findings include indistinct end plates, loss of vertebral height, narrowing of disc space and collapse of vertebra with kyphotic deformity (Figs. 1, 2). The lytic destruction is usually not accompanied by any reactive sclerosis or periosteal reaction [21]. Anterior erosions may be seen if subligamentous involvement occurs. Aneurysmal effects can be seen due to large anterior prevertebral abscess with gouge defects on the anterior and lateral surfaces of the vertebral bodies [19]. Soft tissue changes are seen on plain radiographs but

Fig. 7 Caries L3 vertebra in 10-year-old girl. Sagittal (**a**) and coronal (**b**) post-gadolinium T1-W images reveal destructive lesion in L3 with prevertebral abscess (*arrow* in **a**) and inflammatory changes in bilateral psoas (*arrows* in **b**)

may be missed when the osseous lesions are not visible on radiographs and in cases of posterior element TB [18]. In the thoracic spine, the abscess has a fusiform shape known as the bird's nest appearance. At the thoracolumbar junction, the abscess has an indistinct converging lower border and is known as petering abscess (Fig. 3). In the lumbar region, the psoas outline may be bulging or indistinct on plain radiographs [17]. Radiography has its own disadvantages, with more than 50% bone loss occurring before any radiological changes are evident. The atlanto-occipital and cervicothoracic junctions and posterior elements are also difficult to visualize on plain radiographs.

CT scan readily demonstrates end plate destruction, fragmentation of the vertebrae and pre- and paravertebral abscesses (Figs. 4, 5) [22]. Calcification of the collections and extension of bony fragments and epidural abscess into the spinal canal (Fig. 6) are also better seen on CT scan. It is also useful for guiding percutaneous biopsy and post-drainage follow-up imaging.

With its inherent soft tissue contrast and multiplanar capability, MRI is the optimal imaging modality for evaluating spondylodiskitis. The vertebrae show hypointense signals (relative to muscle) on T1-W images and hyperintense (relative to muscle) on T2-W images with inhomogenous postcontrast enhancement. Hyperintense signal (relative to muscle) on T1 in a chronic disease setting may be considered specific for TB [23]. Disc involvement is seen as destruction of the intervertebral disc space, and in adults there is increased signal of the disc on T2-W images [24]. In a pediatric case series [18], the normal discs were of high signal on T2-W images while the abnormal discs were of low signal intensity. On MRI, there is also superior anatomical delineation of the epidural, paravertebral and intraosseous abscesses and extent of cord and nerve root compromise (Figs. 7, 8). Soft tissue masses may be bilateral and greater than the degree of bone destruction. The paravertebral abscesses may also not correlate with the site of the initial vertebral body lesion. Subligamentous spread of pus in tuberculosis has a smooth margin unlike the pyogenic paravertebral abscesses, which have an irregular margin and may destroy the paraspinal ligaments and surrounding soft tissue [18]. As in adults, tuberculous abscesses in children also commonly show ring peripheral enhancement. However, a few cases of patchy/speckled and diffuse homogenous enhancement have also been described [18]. Cord signal intensity changes are also well appreciated on MRI with high T2 signal within the cord in cases with focal myelitis [2, 21] (Fig. 9). Extradural cord compression may also result in neurological deficit. The anterior subperiosteal (Fig. 10) and nonappendiceal

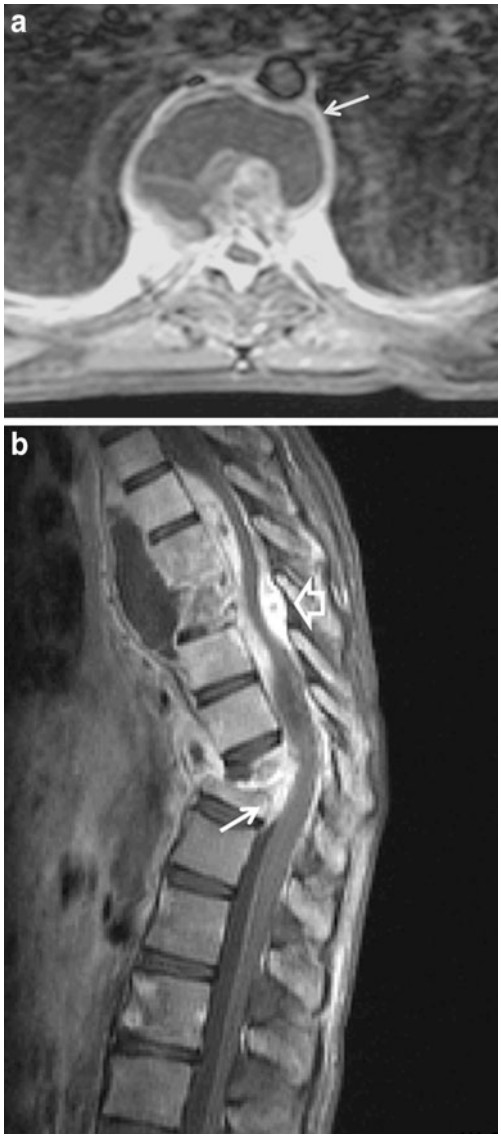

Fig. 8 Axial (**a**) and sagittal (**b**) post-gadolinium images reveal multilevel involvement with heterogenous enhancement, partial collapse, pre- and paravertebral abscess (*arrow* in **a**) anterior (*arrow* in **b**) and posterior (*open arrow* in **b**) epidural abscess with cord compression in a 16-year-old girl with tuberculous spondylitis

tuberculosis (Fig. 11) are also well depicted on MRI. The superior anatomical delineation also helps identify the number of destroyed vertebral bodies against the intact posterior elements (Fig. 12). Signs of healing include regression of a lesion, sclerosis and fusion of contiguous vertebral bodies (Fig. 13) and reduction in the inflammatory soft tissue [19] (Fig. 10).

Differential diagnosis includes pyogenic and fungal infections, other granulomatous diseases and neoplasm particularly neuroblastoma metastases, lymphoma and Ewing sarcoma in children [18].

Fig. 9 Sagittal (**a**) and axial (**b**) T2-W MR images of a 14-year-old boy show partial collapse with anterior wedging of mid-thoracic vertebra (*arrow* in **a**). Hyperintense (relative to muscle) inflammatory soft tissue is seen extending into the pre- and paravertebral space and anterior epidural space. There is evidence of cord compression with hyperintense T2 signal (relative to muscle) within the cord (*arrow* in **b**) that could represent cord edema/myelitis

Clinical profile of insidious onset and chronicity in the setting of an infective pathology favors a diagnosis of TB. In tuberculous spondylitis, there is lack of sclerosis and reactive changes with more rarefaction, large calcified paravertebral abscesses and more destruction and collapse compared with pyogenic form [25]. Slight T1 shortening and inhomogenous enhancement favor tuberculous etiology on MRI.

Brucellar spondylitis favors the lower lumbar spine and is characterized by gas within the disc, minimal paraspinal soft tissue, absence of gibbus deformity and long relaxation time on both T1- and T2-W images.

Fungal disease is difficult to differentiate only on the basis of imaging. Involvement of the posterior elements and rib heads is seen more commonly in fungal infection.

Eosinophilic granuloma should be kept in the differential in case of solitary vertebra involvement, and clinical correlation is essential to differentiate from the central type of TB spondylitis.

Tuberculous arthritis

Tuberculous arthritis can result from contiguous spread (from adjacent metaphyseal lesion) or hematogenous dissemination. Synovial hypertrophy leads to peripheral and central erosions by pressure necrosis [26]. This is followed by subchondral bone and articular cartilage destruction, joint space narrowing being a relatively late complication. Para-articular soft tissue masses, cold abscesses and sinus tracts may develop. Reactive hyperemia results in demineralization and local bone destruction

TB of the joints is characteristically a monoarticular disease, with multifocal disease seen in approximately 10% of patients [27].

The radiographic findings are nonspecific. In the early stage, there is joint widening and soft tissue swelling. This is followed by the appearance of marginal erosions, smudged and indistinct articular cortex and patchy loss of subchondral bone plate (Fig. 14). Phemister's triad of periarticular osteoporosis, peripherally located osseous erosion and gradual diminution of the joint space is highly suggestive of TB of a joint [28]. There is minimal sclerosis and occasional layered periosteal reaction. In children, reactive hyperemia may result in epiphyseal overgrowth with widening of the intercondylar notch from synovitis [2]. Also, damage to the physis in childhood may result in shortening or angulation of the limb. The end stage is fibrous ankylosis compared to the bony ankylosis seen with pyogenic arthritis. Radiographs may not indicate the severity of disease

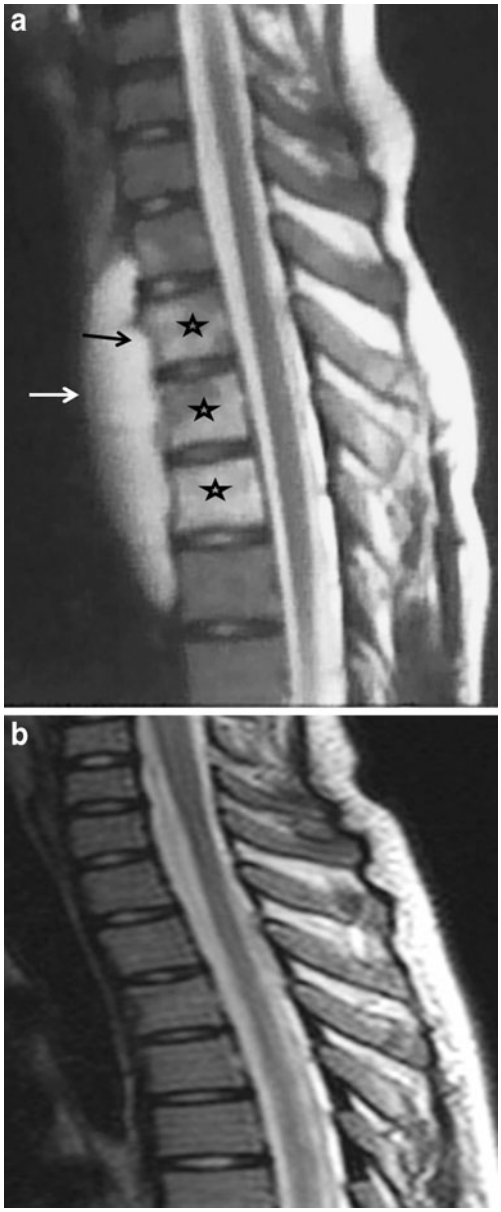

Fig. 10 Anterior subperiosteal caries in a 13-year-old girl. Sagittal (**a**) T2-W image reveals patchy hyperintense signal (relative to muscle) in multiple thoracic vertebra (*stars*), erosions of the anterior cortices (*black arrow*) and a large prevertebral abscess (*white arrow*). Two-year follow-up imaging (**b**) shows complete resolution on this sagittal T2-W image

process in young children with largely unossified epiphyses as cartilage destruction may not be evident on the plain radiograph [29]. There may be anatomical disorganization and destruction of the articular surfaces. In the hip joint, femoral head subluxation or dislocation may be seen. Occasionally, the femoral capital epiphysis may get flattened and sclerotic with appearance similar to Perthe disease (Fig. 15).

US is useful to evaluate for synovial thickening and joint effusion and for guided aspiration (Fig. 16).

CT scan demonstrates well the lesion extent, osseous destruction and associated soft tissue abscesses. It is especially useful in bones not well evaluated by radiographs, like sternum, scapula and sacroiliac joints.

MRI is the imaging modality of choice for early detection of joint TB. Synovial proliferation (Figs. 17, 18) is seen as intermediate signal intensity on T1 (relative to muscle) and intermediate to high signal intensity on T2-W images. However, hypointense signal (relative to muscle) is obtained on T2-W images in 40% of cases. This is probably due to fibrosis, macrophage infiltration and free radicals, perilesional cellular infiltrate and high lipid content. Biphasic pattern of active pannus (enhances postcontrast) and chronic fibrotic nonenhancing pannus is characteristic for TB arthritis [30]. Articular erosions and subchondral bone destruction along with bone marrow edema are also well seen (Fig. 19). Soft tissue abnormalities such as myositis (Fig. 20), cellulitis, para-articular abscess formation, tenosynovitis, bursitis and sinus tract formation are well delineated on the short tau inversion recovery (STIR) and postcontrast sequences (Figs. 21, 22) [1]. Sacroiliac joints are also well evaluated by MRI (Fig. 23). A disease of young adults, sacroiliac joint tuberculosis has also been reported occasionally in children [29, 31].

The differentials include pyogenic, haemophiliac and juvenile rheumatoid arthritis. Monoarticular arthritis with insidious onset of symptoms and gradual progression favor a diagnosis of tuberculosis. Definitive diagnosis requires aspiration or synovial biopsy.

Tuberculous tenosynovitis

Primary tuberculous tenosynovitis is an extremely rare condition and most commonly involves the flexor tendon sheaths of the hand. US reveals tendon and synovial thickening with relatively little effusion. MRI shows the extent of soft tissue involvement and any associated osseous or joint disease [1].

Tuberculous bursitis

The trochanteric, subacromial, subgluteal and radioulnar wrist bursae are most commonly affected. On MRI, there may be a uniform distension of the bursa or multiple small abscesses within the bursa. Caseous necrosis and fibrotic material within the fluid-filled bursa may result in low signal intensity on T2-W images [1].

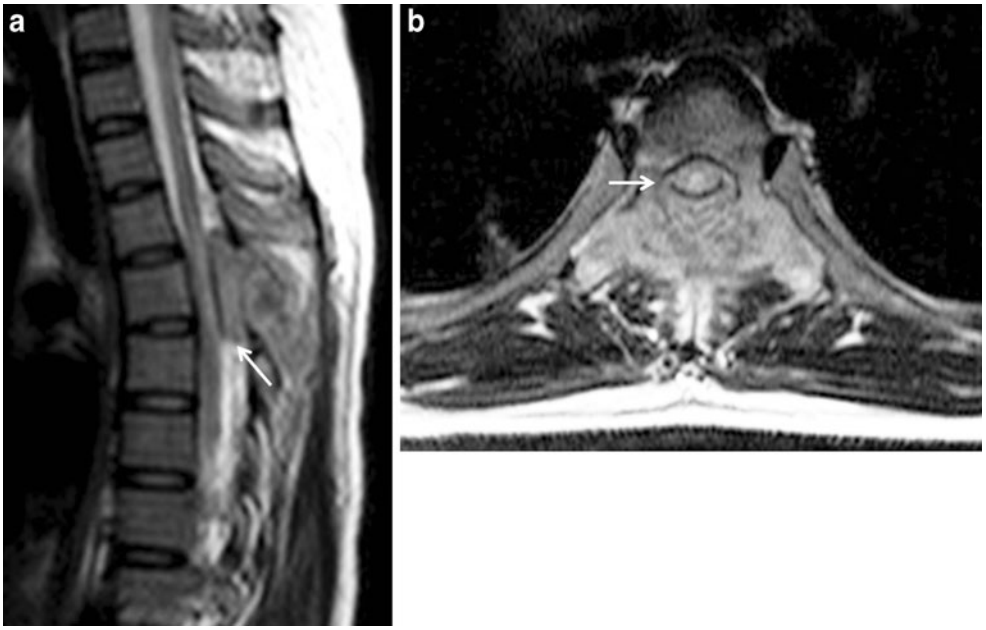

Fig. 11 A 13-year-old girl with thoracic nonappendiceal tuberculosis. Sagittal T2-W image (**a**) shows altered signal intensity of spinous process of T6 and T7 vertebra with thoracic epidural soft tissue mass (*arrow*) and cord compression. Axial T2-W image (**b**) reveals hyperintensity in bilateral laminae, pedicles and transverse processes and spinous process of T6 vertebra with cord compression and altered cord signal intensity (*arrow*)

Fig. 12 Sagittal T2 image of a 5-year-old girl with cervicothoracic TB spondylitis reveals multiple contiguous vertebral body collapse (C7 to T3). There is a hyperintense (relative to muscle) soft tissue mass extending prevertebrally and intraspinally. The large ventral epidural abscess is seen compressing the thecal sac and lifting the cord (*open arrow*). The spinous processes of the destroyed vertebrae appear to be of normal signal intensity (*arrows*)

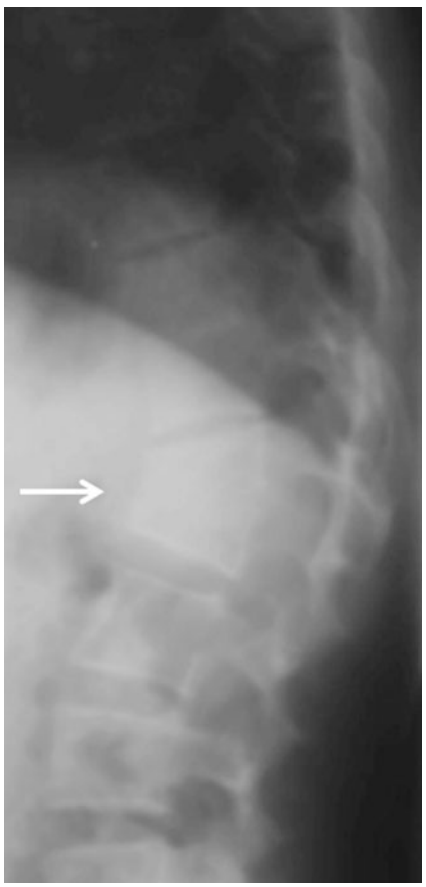

Fig. 13 Lateral radiograph of a 21-year-old man with a history of tuberculous spondylitis in childhood shows anterior wedging and osseous block vertebrae T12 and L1 (*arrow*) with kyphotic deformity-healed tuberculosis

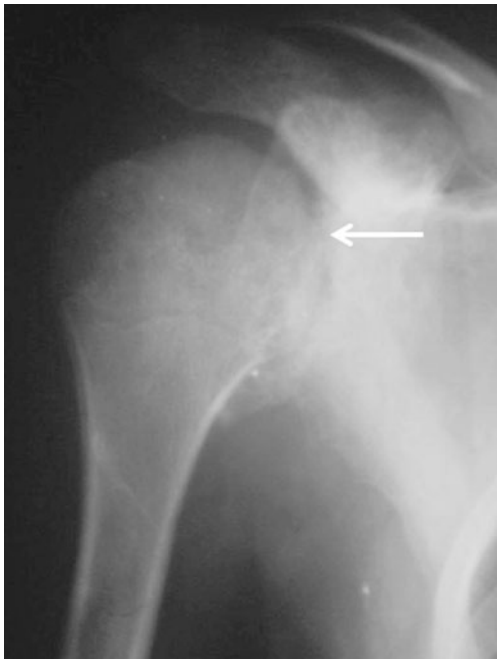

Fig. 14 AP radiograph of right shoulder shows subarticular lysis (*arrow*), marginal erosions and joint space narrowing in a 16-year-old boy with right shoulder tuberculosis

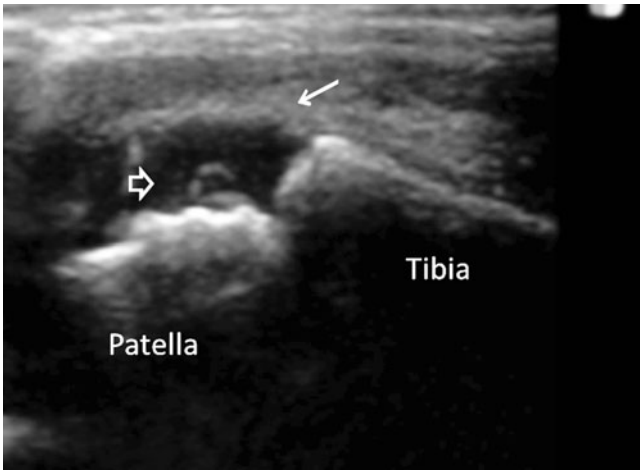

Fig. 16 US image of the knee in the sagittal plane shows synovial hypertrophy (*arrow*) and joint effusion (*open arrow*) in a 10-year-old boy with left knee tuberculosis

Tuberculous osteomyelitis

The disease is usually monostotic in adults; however, multiple sites of involvement are usually seen in children [29].

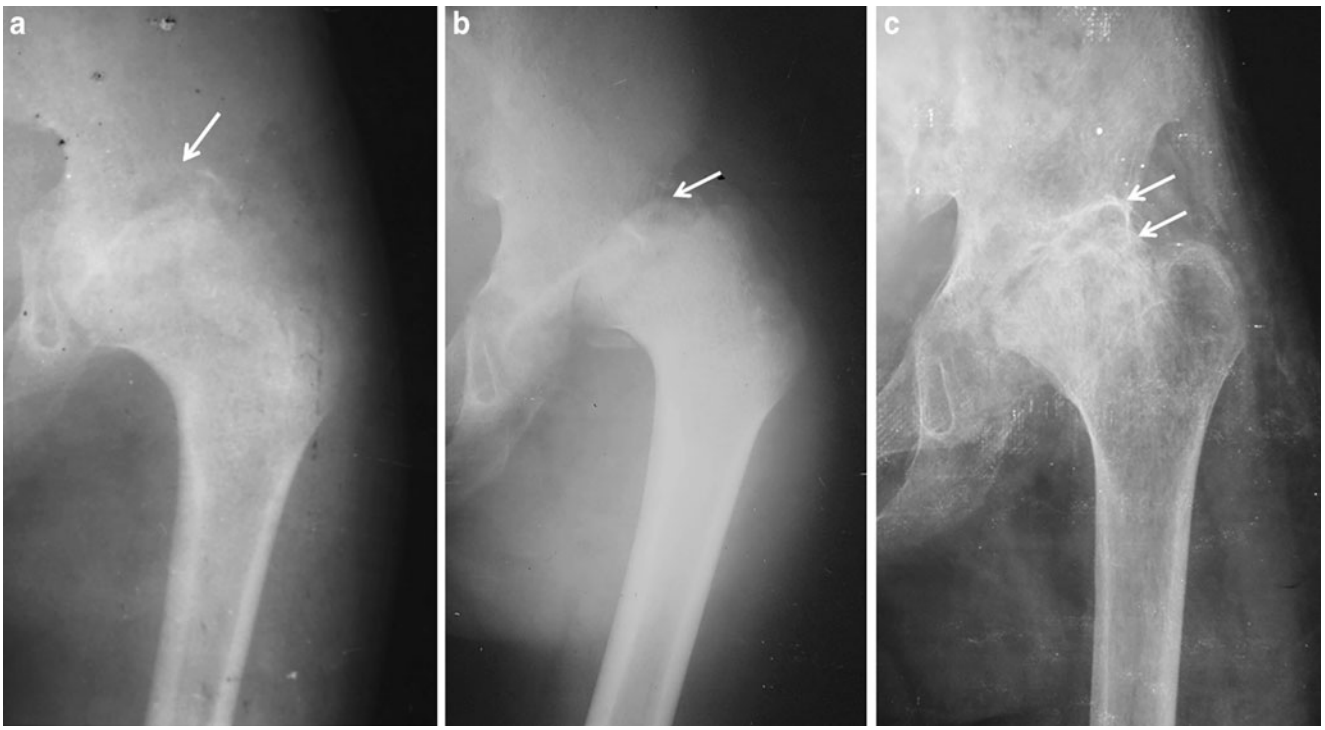

Fig. 15 Hip tuberculosis in a 12-year-old boy. **a** Initial radiograph at presentation shows juxta-articular osteopenia and reduction in joint space (*arrow*). **b** Radiograph obtained 4 months later shows upward displacement of femoral head with mild flattening (*arrow*) and soft tissue swelling. **c** One-year follow-up radiograph reveals flattening of femoral head, subchondral lytic foci in acetabulum and femoral head (*arrows*) and reduced joint space

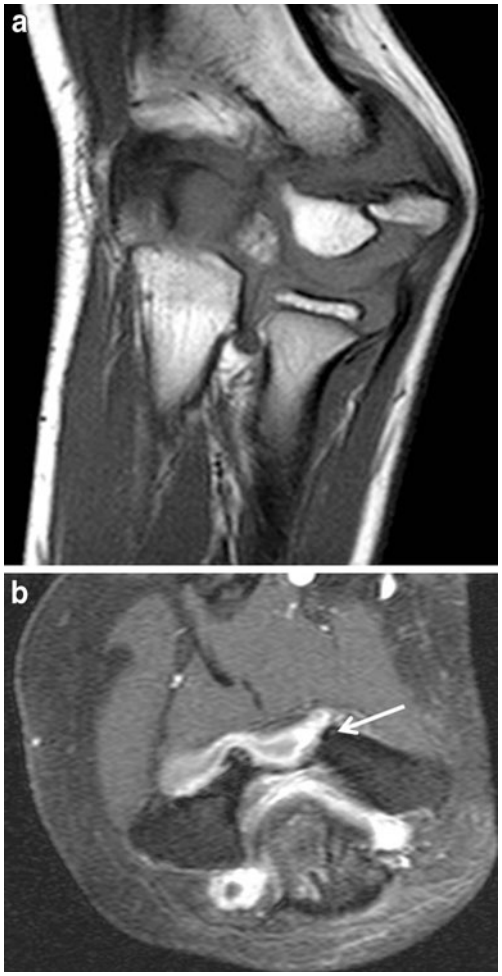

Fig. 17 Coronal T1-W image (**a**) and axial post-gadolinium T1-W image (**b**). Marked synovial hypertrophy is seen in synovitis stage of elbow tuberculosis in a 14-year-old girl. Diffuse enhancement of the intra-articular abnormality (*arrow* in **b**) suggests synovitis as effusion does not enhance

Fig. 18 Sagittal post-gadolinium T1-W image (**a**) and coronal STIR (**b**) reveal cartilage loss (*arrow* in **a**), bursitis (*open arrow* in **a**), enlarged popliteal lymph nodes (*arrowhead* in **a**) and anatomical disorganization (*arrow* in **b**) in knee tuberculosis in a 3-year-old boy

The bones of the extremities are most commonly involved, including the small bones of the hands and feet. It is caused by hematogenous spread from an active focus—pulmonary, meningeal or lymphatic.

The initial lesion on plain radiograph is an eccentric area of osteolysis in the metaphysis. This may be accompanied by soft tissue swelling and subtle periosteal reaction. Transphyseal spread of the lytic focus (Figs. 24 and 25) is characteristic for tuberculosis and is not seen in pyogenic infection [21, 32]. Sclerosis and sequestration are relatively uncommon. Occasionally, an infiltrative pattern of TB osteomyelitis may be seen in children [29]. Ribs are occasionally involved and show irregular lytic destruction (Fig. 26) and may be associated with extrapleural soft tissue thickening and abscesses The differentials include pyogenic and fungal infection and clinical correlation is necessary.

CT scan better delineates the bony destruction and extent of soft tissue involvement. It is also better for evaluating

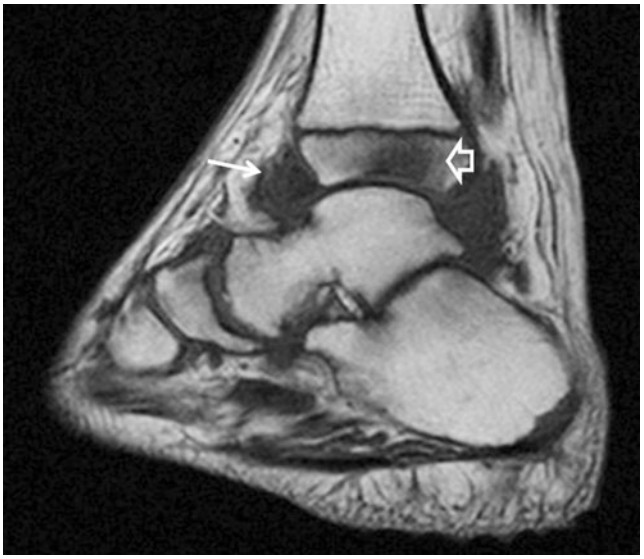

Fig. 19 Ankle tuberculosis in a 12-year-old boy. Pre-gadolinium sagittal T1-W image shows cortical irregularity, joint space loss, synovitis (*arrow*) and marrow edema (*open arrow*)

bones like the sacrum and sternum (Fig. 27). MRI may demonstrate intraosseous involvement earlier than the other imaging modalities. An area of altered marrow signal intensity with irregular margins, cortical breach and ill-defined soft tissue is suspicious for tuberculous osteomyelitis on MRI

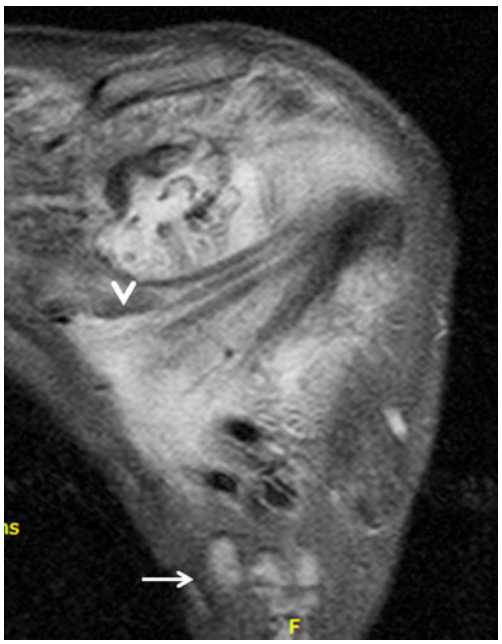

Fig. 20 Coronal STIR image shows hyperintense signal (relative to muscle) in the subcutaneous tissues and muscle (myositis) (*arrowhead*) with enlarged axillary lymph nodes (*arrow*) in a case of shoulder tuberculosis in a 13-year-old boy

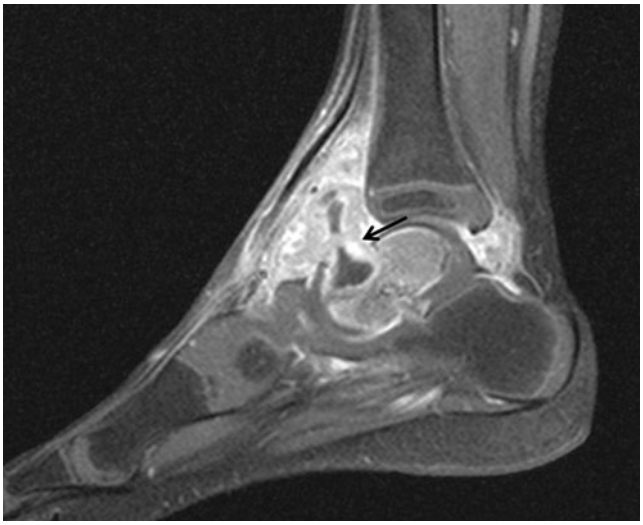

Fig. 21 Sagittal post-gadolinium T1-W image shows rim-enhancing abscess (*arrow*) and inflammatory tissue in the synovium, bone and soft tissue in a 7-year-old boy with foot and ankle tuberculosis

[1]. Associated sinus tracts, fistulae and abscesses are better delineated on the gadolinium-enhanced images (Fig. 28).

Fig. 22 Hip tuberculosis in an 8-year-old girl. Sagittal post-gadolinium T1-W image reveals synovitis (*arrow*) with periarticular abscess (low signal soft tissue with rim enhancement) formation (*open arrow*)

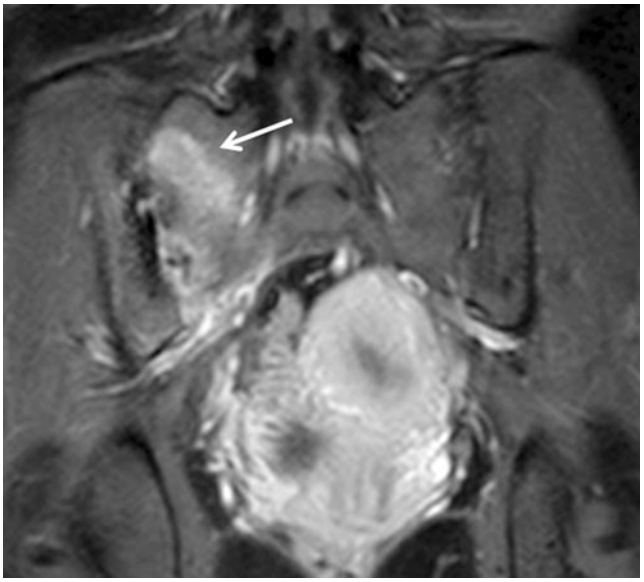

Fig. 23 Coronal post-gadolinium T1-W image reveals abnormal subarticular marrow enhancement (*arrow*) and joint irregularity of the right sacroiliac joint in a 17-year-old girl with right tuberculous sacroilitis

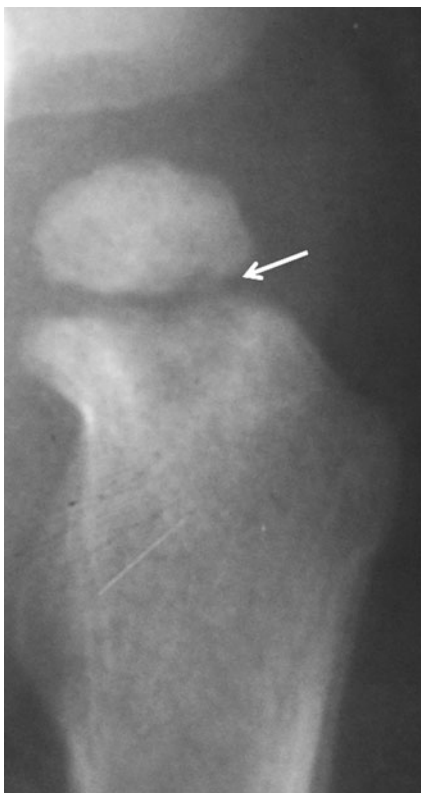

Fig. 24 Transphyseal spread in tuberculosis. Metaphyseal focus in the proximal femur shows extension across the physeal line into the epiphysis (*arrow*) in the AP radiograph of the left hip of a 4-year-old boy

Fig. 25 Pre-gadolinium T1-W image shows hypointense signal (relative to muscle) in epimetaphyseal region (*arrow*) of the left femur and adjacent soft tissue. Note the characteristic transphyseal spread in a case of tuberculous osteomyelitis in a 7-year-old boy

Cystic TB

Multifocal tuberculous osteomyelitis, also known as osteitis cystica tuberculosa multiplex, is an unusual pattern of TB

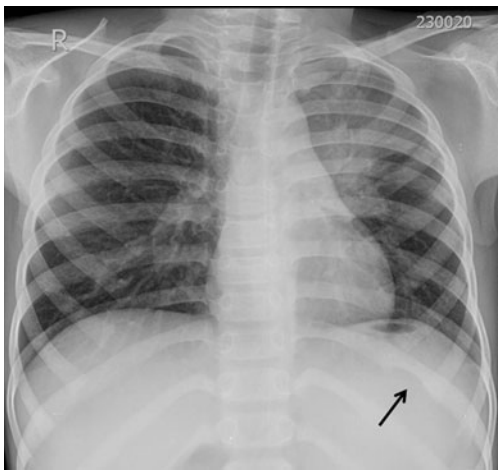

Fig. 26 Tuberculous osteomyelitis in the left tenth rib. Chest PA radiograph of a 15-year-old boy with pulmonary tuberculosis who presented with fluctuant soft tissue lower chest wall swelling. There is irregular lytic destruction in the inferior aspect of posterior left tenth rib (*arrow*) and left upper zone consolidation

Fig. 27 CT pelvis (coronal reformatted image) in an 18-year-old girl with disseminated tuberculosis shows multiple osseous lytic lesions involving of the bilateral ilia and sacrum (*arrows*)

osteomyelitis more commonly seen in children. It is characterized by multiple small, well-defined oval lytic lesions of variable size that usually lack sclerotic margins (Fig. 29). The metaphyses of long bones are

Fig. 28 Coronal post-gadolinium T1-W image reveals abnormal intra- and extraosseous enhancement with periosteitis (*arrow*) and soft tissue collections in tuberculous involvement in the left tibia in a 16-year-old boy

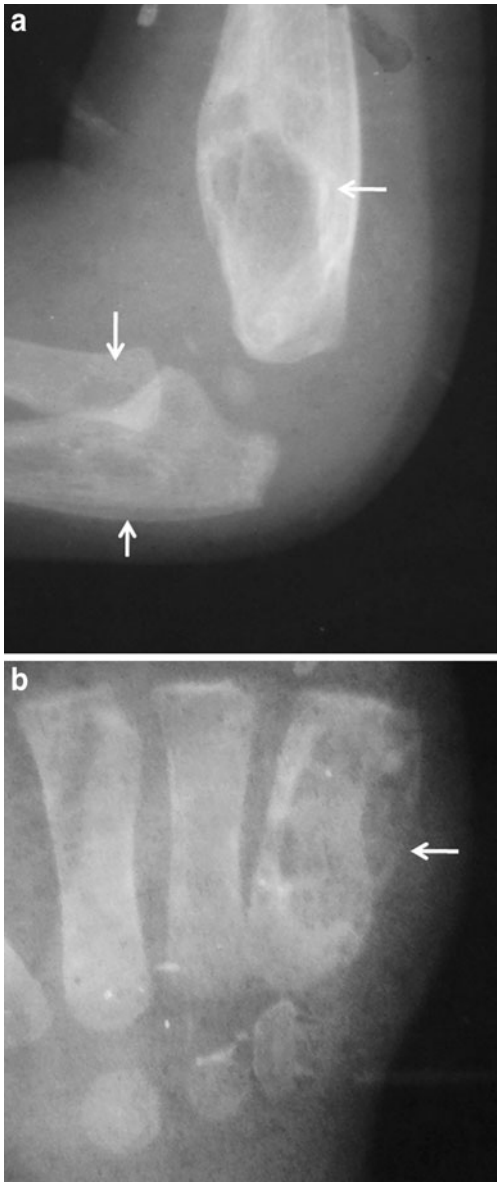

Fig. 29 Multifocal tuberculous osteomyelitis in a 4-year-old girl. **a** Lateral radiograph of the elbow shows multiple, well-defined lytic lesions of variable size in the metaphyses of the humerus, radius and ulna (*arrows*) with soft tissue swelling. **b** Expansile lytic lesion with cortical thinning and soft tissue swelling of the left fifth metacarpal (*arrow*) seen in the AP radiograph of the hand of same patient

affected and mild metaphyseal expansion may be seen [1, 33].

Tuberculous dactylitis

Tuberculous involvement of the short tubular bones of the hands and feet is also more common in children. Spina

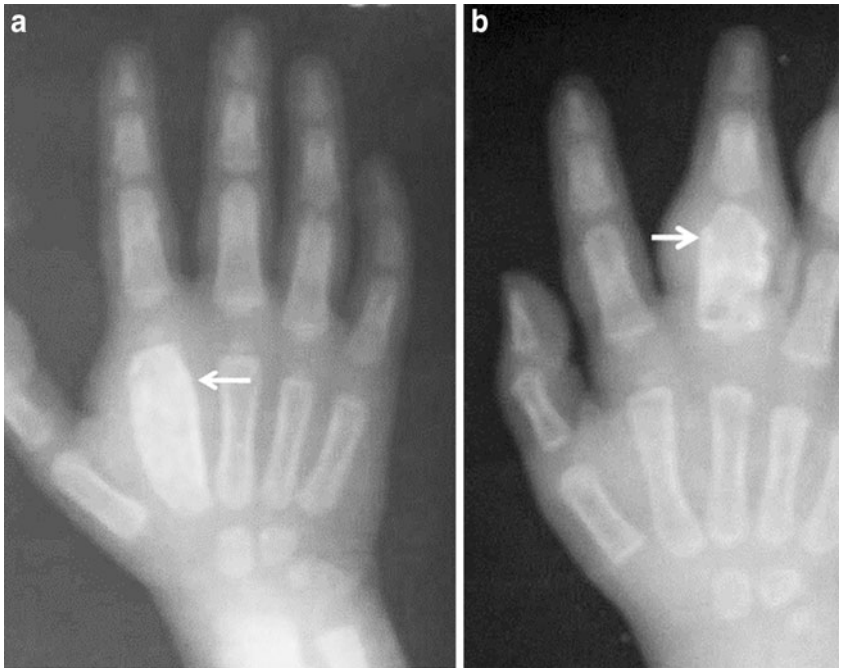

Fig. 30 Tuberculous dactylitis in two different 3-year-old boys. AP radiograph shows expansile lysis (spina ventosa) with cortical thinning and soft tissue swelling of the second metacarpal (*arrow* in **a**) and third proximal phalanx (*arrow* in **b**)

ventosa (a spine-like projection puffed with air) is the term used to describe the ballooned-out appearance of the bone with an internal cyst-like cavity (Fig. 30). Pronounced fusiform soft tissue swelling with periosteal thickening and bone destruction is seen [21, 32]. Sequestration, sinus tracts and bony expansion may also be seen in children [21].

Calvarial tuberculosis

Calvarial tuberculosis is a rare presentation that usually involves the frontal and parietal bones because the presence of large amounts of cancellous bone. It may present as a subgaleal swelling or a discharging sinus when the outer table of the cranium is involved. Inner table disease is usually associated with extradural granulation tissue. Three types of lesions have been described on plain radiographs: perforating, diffuse and sclerotic form [34]. The lytic lesions may demonstrate central sclerotic focus also known as button sequestrum. CT demonstrates soft tissue swelling, bony destruction and spread of the disease process to the extradural space, meninges and brain parenchyma.

Petrous tuberculosis

Involvement of petrous bone by tuberculosis has been occasionally reported. Two forms have been described: circumscribed and infiltrating type [35]. CT demonstrates well the extent of bony involvement and MRI better delineates the associated soft tissue component.

Conclusion

The diagnosis of pediatric musculoskeletal tuberculosis is difficult and requires a high index of clinical suspicion. It has no pathognomonic signs and needs to be differentiated from pyogenic and fungal infections, granulomatous diseases and neoplasms. On the basis of the pattern of bone involvement and imaging features, the radiologist should alert the clinician to the possibility of TB in the appropriate clinical setting. Early institution of anti-tuberculous therapy can lead to resolution and help decrease morbidity.

References

1. De Backer AI, Vanhoenacker FM, Sanghvi DA (2009) Imaging features of extraaxial musculoskeletal tuberculosis. Indian J Radiol Imaging 19:176–186
2. Moore SL, Rafii M (2001) Imaging of musculoskeletal and spinal tuberculosis. Radiol Clin North Am 39:329–342
3. Rasool MN (2001) Osseous manifestations of tuberculosis in children. J Pediatr Orthop 21:749–755
4. Kumar R (2005) Spinal tuberculosis: with reference to the children of Northern India. Childs Nerv Syst 21:19–26
5. Westall J (1997) Tuberculosis levelling off worldwide. BMJ 314:921
6. Engin G, Acunas B, Acunas G et al (2000) Imaging of extrapulmonary tuberculosis. Radiographics 20:471–488
7. Davidson P, Horowitz I (1970) Skeletal tuberculosis. A review with patient presentations and discussion. Am J Med 48:77–84
8. Weaver P, Lifeso R (1984) The radiological diagnosis of tuberculosis of the adult spine. Skeletal Radiol 12:178–186
9. Ranson M (2009) Imaging of pediatric musculoskeletal infection. Semin Musculoskelet Radiol 13:277–299

10. Soler R, Rodriguez E, Rumuinan C et al (2001) MRI of musculoskeletal extraspinal tuberculosis. J Comput Assist Tomogr 25:177–183
11. Boussel L, Marchand B, Blineau N et al (2002) Imaging of osteoarticular tuberculosis. J Radiol 83:1025–1034
12. Shanley DJ (1995) Tuberculosis of the spine: imaging features. AJR 164:659–664
13. Jaovisidha S, Chen C, Ryu KN et al (1996) Tuberculous tenosynovitis and bursitis: imaging findings in 21 cases. Radiology 201:507–513
14. Suh JS, Lee JD, Cho JH et al (1996) MR imaging of tuberculous arthritis: clinical and experimental studies. J Magn Reson Imaging 6:185–189
15. Martini M, Adjrad A, Boudjemaa A (1986) Tuberculous osteomyelitis: a review of 125 cases. Int Orthop 10:201–207
16. Sharif HS, Morgan JL, Al Shahed MS et al (1995) Role of CT and MR imaging in the management of tuberculous spondylitis. Radiol Clin North Am 33:787–804
17. Bhan S, Nag HL (2001) Skeletal tuberculosis. In: Sharma SK, Mohan A (eds) Tuberculosis, 1st edn. Jaypee, New Delhi, pp 237–260
18. Andronikou S, Jadwat S, Douis H (2002) Patterns of disease on MRI in 53 children with tuberculous spondylitis and the role of gadolinium. Pediatr Radiol 32:798–805
19. Dixit R (2005) Tuberculosis of the spine. In: Berry M, Chowdhury V, Mukhopadhyay S et al (eds) Diagnostic radiology- musculoskeletal and breast imaging, 2nd edn. Jaypee, New Delhi, pp 111–129
20. Hoffman EB, Crosier JH, Cremin B (1993) Imaging in children with spinal tuberculosis. A comparison of radiography, computed tomography and magnetic resonance imaging. J Bone Joint Surg Br 75:233–239
21. Yao D, Sartoris D (1995) Musculoskeletal tuberculosis. Radiol Clin North Am 33:679–689
22. Naim-Ur-Rahman JA, Jamjoom ZA et al (1997) Neural arch tuberculosis: radiological features and their correlation with surgical findings. Br J Neurosurg 11:32–38
23. Maiuri F, Iaconetta G, Gallicchio B et al (1997) Spondylodiscitis. Clinical and magnetic resonance diagnosis. Spine 22:1741–1746
24. Loke TK, Ma HT, Chan CS (1997) Magnetic resonance imaging of tuberculous spinal infection. Australas Radiol 41:7–12
25. Tan KP, Thomas A (1987) Radiologically guided percutaneous needle biopsy of vertebral and paravertebral lesions. Singapore Med J 28:42–52
26. Morris BS, Varma R, Garg A et al (2002) Multifocal musculoskeletal tuberculosis in children: appearances on computed tomography. Skeletal Radiol 31:1–8
27. De Vuyst D, Vanhoenacker F, Gielen J et al (2003) Imaging features of musculoskeletal tuberculosis. Eur Radiol 13:1809–1819
28. De Backer AI, Mortele KJ, Vanhoenacker FM et al (2006) Imaging of extraspinal musculoskeletal tuberculosis. Eur J Radiol 57:119–130
29. Teo HE, Peh WC (2004) Skeletal tuberculosis in children. Pediatr Radiol 34:853–860
30. Sawlani V, Chandra T, Mishra RN et al (2003) MRI features of tuberculosis of peripheral joints. Clin Radiol 58:755–762
31. Soholt ST (1951) Tuberculosis of the sacroiliac joint; A review of 75 cases. J Bone Joint Surg Am 33(A:1):119–130
32. Harisinghani MG, McLoud TC, Shepard JA et al (2000) Tuberculosis from head to toe. Radiographics 20:449–470
33. Burrill J, Williams CJ, Bain G et al (2007) Tuberculosis: a radiologic review. Radiographics 27:1255–1273
34. Ray M, Kataria S, Singhi P (2002) Unusual presentation of disseminated tuberculosis. Indian Pediatr 39:88–91
35. Kumar S, Puri V, Malik R et al (1991) Tuberculosis of petrous apex. Indian Pediatr 28:407–409